Carbohydrate Polymers 93 (2013) 279–284

Contents lists available at SciVerse ScienceDirect

Carbohydrate Polymers

journal homepage: www.elsevier.com/locate/carbpol

Curcumin/xanthan–galactomannan hydrogels: Rheological analysis and biocompatibility

Eneida Janiscki Da-Lozzo[a,c], Ricardo Cambaúva Andrukaisti Moledo[a,c], Cloris Ditzel Faraco[b], Claudia Feijó Ortolani-Machado[b], Tania Mari Bellé Bresolin[d], Joana Léa Meira Silveira[a,*]

[a] Departamento de Bioquímica e Biologia Molecular, UFPR, B.P. 19046, Centro Politécnico, Cep. 81531-990, Curitiba (PR), Brazil
[b] Departamento de Biologia Celular, UFPR, Curitiba, Brazil
[c] Centro de Ciências Biológicas e Saúde, PUC Paraná, Curitiba, Brazil
[d] Curso de Farmácia, Núcleo de Investigações Químico-Farmacêuticas (NIQFAR), Universidade do Vale do Itajaí – UNIVALI, Itajaí, Brazil

ARTICLE INFO

Article history:
Received 17 October 2011
Received in revised form 9 February 2012
Accepted 17 February 2012
Available online 7 March 2012

Keywords:
Xanthan–galactomannan
Hydrogel
Curcumin
Chick embryo chorioallantoic membrane
Biocompatibility
Dynamic rheological analysis

ABSTRACT

Curcumin, a lipophilic compound found in the plant *Curcuma longa* L., exhibits a wide range of pharmacological activity; however, its therapeutic use has been limited because of its low bioavailability following oral administration. The aim of this study was to evaluate the viscoelastic characteristics and biocompatibility of a curcumin/xanthan:galactomannan hydrogel (X:G) system after topical application on chick embryo chorioallantoic membrane (CAM), a system established with a view toward curcumin nasal or topical pharmaceutical applications or possible administration in cosmetics or foods. A rheological analysis indicated that incorporation of curcumin did not alter the viscoelastic characteristics of the X:G hydrogel, suggesting that there was no change in the structure of the gel network. X:G hydrogels did not induce CAM tissue injury and the curcumin/X:G hydrogel system was also highly biocompatible. We conclude that the X:G hydrogel represents a potential matrix for curcumin formulations.

1. Introduction

Curcumin, a lipophilic compound found in the plant *Curcuma longa* L., has traditionally been used as a yellow pigment to color food and cosmetics (Jayaprakasha, Jagan Mohan Rao, & Sakariah, 2005). Curcumin possesses a wide range of pharmacological properties, including antioxidant (Miquel, Bernd, Sempere, Díaz-Alperi, & Ramírez, 2002), anti-inflammatory (Shakibaei, John, Schulze-Tanzil, Lehmann, & Mobasheri, 2007; Sharma, Gescher, & Steward, 2005; Xu, Deng, Chow, Zhao, & Hu, 2007), anti-angiogenic (Gururaj, Belakavadi, Venkatesh, Marmé, & Salimath, 2002), antitumor (Dorai & Aggarwal, 2004; Gafner et al., 2004; Kunnumakkara, Anand, & Aggarwal, 2008; Shishodia, Chaturvedi, & Aggarwal, 2007; Singh & Agarwal, 2003), and immunomodulatory (Srivastava, Singh, Dubey, Misra, & Khar, 2011) activities. Despite this large spectrum of biological activity, the therapeutic use of curcumin has been limited because of its low bioavailability when administered orally (Sharma et al., 2005). Thus, the development of alternative strategies for curcumin topical use could open up new possibilities for the development of medicinal applications.

Polymeric hydrogels are being increasingly studied as release matrices (Peppas, Bures, Leobandung, & Ichikawa, 2000). Polysaccharide hydrogels have been widely employed in various industrial and pharmaceutical applications. The polysaccharides xanthan (X) and galactomannan (G) alone are simple water-soluble thickening agents, but when they are mixed, an original gelation occur (Dea & Morrison, 1975). The galactomannan from the seeds of *Mimosa scabrella* Bentham used in xanthan:galactomannan (X:G) binary system has been tested as a hydrophilic matrix for the release of theophylline (Ughini, Andreazza, Ganter, & Bresolin, 2004) and sodium diclofenac (Vendruscolo, Andreazza, Ganter, Ferrero, & Bresolin, 2005) in the form of directly compressed tablets and capsules as well as hydrogel matrix to stabilize ascorbic acid (Koop, Praes, Reicher, Petkowicz, & Silveira, 2009). A system of xanthan and locust bean gum was studied as a hydrogel matrix to stabilize emulsions (Makri & Doxastakis, 2006). Considering the natural source of each of the individual components, a curcumin/X:G hydrogel system could have a variety of applications in food, cosmetic, and pharmaceutical industries. However, when a water-insoluble drug like curcumin is added to a hydrogel, it can only be dispersed, not dissolved; thus, a transparent aqueous gel cannot be obtained (Knighton, Ausprunk, Tapper, & Folkman, 1977; Peppas et al., 2000). Water-insoluble drugs are often dissolved in water miscible co-solvents, such as ethanol, before being added to the gel. Although the addition of ethanol to the gel could potentially

* Corresponding author. Tel.: +55 41 3361 1665; fax: +55 41 3266 2042.
E-mail addresses: jlms12@yahoo.com, jlms12@ufpr.br (J.L.M. Silveira).

0144-8617/$ – see front matter © 2012 Elsevier Ltd. All rights reserved.
doi:10.1016/j.carbpol.2012.02.036

precipitate polysaccharides, the OH group of the alcohol also helps to maintain a certain degree of hydrophilicity and thereby prevents precipitation (Montembault, Viton, & Domard, 2005). Another possible outcome of directly dissolving lipophilic drug molecules in a hydrogel mixture is that these drug molecules might be hosted within the three-dimensional gel network and lose their functionality. Accordingly, both rheological properties and biocompatibility of the curcumin/X:G hydrogel system must first be assessed.

The avian chorioallantoic membrane (CAM), the outermost extra-embryonic membrane lining the noncellular eggshell membrane, is one of the most commonly used models for studying angiogenic and anti-angiogenic effects (Eun & Koh, 2004; Hazel, 2003; Knighton et al., 1977; Nguyen, Shing, & Folkman, 1994). It has also been used as an *in vivo* model for evaluating tissue responses to biomaterials (Klueh, Dorsky, Moussy, & Kreutzer, 2003; Valdes, Kreutzer, & Moussy, 2002) and for assessing the biocompatibility of drug-delivery systems after topical administration on the CAM surface (Vargas, Zeisser-Labouèbe, Lange, Gurny, & Delie, 2007). The inflammatory response of the CAM to biomaterials is similar to that observed in mammalian models (Klueh et al., 2003; Valdes et al., 2002). This *in vivo* model enables constant observation of the site of the implant, providing rapid, simple, and low-cost monitoring.

The biocompatibility of the curcumin X:G hydrogel system has not yet been evaluated. Therefore, the aims of this study were to determine the rheological properties of curcumin/X:G hydrogels and verify their biocompatibility using the CAM model.

2. Materials and methods

2.1. Materials

Xanthan, curcumin, and galactomannan from locust bean gum (Man:Gal 3.5:1) were obtained from commercial suppliers (Sigma–Aldrich, Co, St Louis, MO, USA). The mannose:galactose (Man:Gal) ratio of galactomannan was determined by gas liquid chromatography (GLC) and ^{13}C NMR spectroscopy (Ganter & Reicher, 1999). PLLA (poly-L-lactide acid) resin was obtained from Birmingham Polymers (MW 13.7 kDa; Birmingham, AL, USA).

2.2. Preparation of the X:G hydrogel

Aqueous solutions of xanthan (X) and galactomannan (G) were prepared and then blended at 80 °C with mechanical stirring to obtain a X:G hydrogel (1:1) with a total polysaccharide concentration of 12.5 g/L. A 50-μL aliquot of a 10-mg/mL curcumin solution in ethanol was added to the xanthan solution prior to blending to obtain a X:G hydrogel containing 0.5 mg/mL of curcumin. X:G hydrogels were stored at 4 °C before analysis.

2.3. Preparation of PLLA films

A 1% solution (w/v) of PLLA was prepared by dissolving PLLA resin in chloroform overnight. Four milliliters of solution was used to cast a thin PLLA film on cleaned glass Petri dishes (55 × 20 mm). The solvent was allowed to evaporate slowly in air, ensuring the formation of a smooth, non-porous film (55 mm diameter, 0.02 mm thickness). The cast film was rinsed with deionized water, air-dried, and then kept under vacuum to remove any residual solvent (Nguyen et al., 2004). For sterilization, the PLLA-coated dish was exposed to UV irradiation for 45 min prior to the experiment.

2.4. Dynamic rheological analysis

Dynamic oscillatory measurements were performed using a dynamic stress rheometer (model Haake RS75) equipped with a PP35Ti sensor (plate, 35 mm in diameter). The temperature was controlled by a circulating water bath and maintained at 25 °C with a thermoelectric Peltier device. Small deformation oscillatory experiments were conducted in two stages: (1) deformation sweeps at constant frequency (1 Hz) to determine the maximum deformation attainable by the sample in the linear viscoelastic range and (2) frequency sweeps (0.01–10 Hz) at a constant deformation (1% strain) within the linear viscoelastic range. Mechanical spectra were obtained by recording the dynamic moduli (G' and G") and η^* as a function of frequency. G' is the dynamic elastic or storage modulus, which is related to the material response as a solid; G" is the dynamic viscous or loss modulus, which is related to the material response as a fluid; and η^* is the dynamic viscosity, which approaches zero-shear viscosity as both the shear rate and the frequency of deformation are reduced to zero. All tests were done at least three times, and mean and standard error values were calculated. The dynamic rheological studies were performed for X:G hydrogel samples (12.5 g/L total polysaccharide concentration) containing 0.10–0.50 mg/mL curcumin and without added curcumin.

2.5. Release experiments

Drug release was assessed in dissolution studies performed in triplicate using a USP rotating basket method. The hydrogel system (10 mL) containing 0.5 mg/mL of curcumin was placed into the basket. The dissolution media was 300 mL of isotonic phosphate buffer, pH 7.4, maintained at 37 °C and agitated at 50 rpm. At appropriate intervals, 1-mL aliquots of dissolution medium were withdrawn and assayed for drug release and replaced with 1 mL of fresh buffer. The aliquots were filtered through cellulose acetate membranes (0.45 μm) and evaporated under vacuum (Speed Vac) at 20 °C. Precipitates were dissolved in 0.5 mL ethanol, ultrasonicated for 10 min in ice-cold water, and centrifuged at 10,000 rpm for 20 min. Supernatant samples were assayed by fluorescence spectrophotometry (RF-5301 PC, Shimadzu) with excitation and emission wavelengths of 420 and 530 nm, respectively, and a 5-nm slit width. Dissolution medium without sample treated in the same manner as samples was used as a blank. A standard curve was generated by preparing serial dilutions of a stock solution of curcumin (5 mg/mL) in ethanol and then adding to dissolution medium to yield samples of curcumin in a concentration range of 2.5–500 ng/mL. Curcumin standards were assayed in triplicate in the same manner as samples. The emission intensity of samples at 530 nm was plotted against curcumin concentration. After linear regression analysis, the slopes, intercepts and the correlation coefficients (r) of curves were calculated using Excel 5.0 software.

2.6. CAM assay

Fertilized chicken eggs were obtained from a local hatchery. The eggs were cleaned with a 70% ethanol solution and incubated at 37 °C and 60% relative humidity. On day 5 of development, the surface of each egg was sterilized and part of the CAM containing the central vein was exposed by aseptically opening a circular window in the egg shell under a laminar flow hood. Test substances (50 μL X:G hydrogel with and without 50 μg curcumin) were applied from above onto the developing CAMs. A PLLA film (0.25 cm^2) was used as a positive control. The window was sealed with sterile plastic tape, and the eggs were returned to the incubator. On day 13 of incubation, the windows were extended to a diameter of about 3 cm, and the response to the different tested materials was analyzed by gross evaluation and histological analysis. Embryos that did not survive or in which disks could not be located were not included in the results.

2.7. Gross evaluation and analysis of angiogenesis in CAM assays

The macroscopic appearance of CAMs was examined under an Olympus SZ40 stereomicroscope coupled to a digital camera (Sony 7.2 No. DSC-W7). The CAMs were photographed *in ovo*. Incorporation of the implanted biomaterial was evaluated and erythema and opacity were assessed as described previously (Klueh et al., 2003). Angiogenesis was analyzed using Image-Pro Plus software version 4.5 by calculating the vascular density index (VDI), which represents the number of intersections made by blood vessels (arterioles and venules) with a square grid containing nine smaller squares superimposed on the micrographs (Yang et al., 2005). Vessels were counted in four sites in the square grid at a 4× final magnification. VDI in different implants was calculated and plotted as a percentage of that in controls (VDI%) (Roy et al., 2006). For each group (each type of biomaterial implanted) at least six replicates (n) were used. Statistical analyses were performed using Student's t-tests.

2.8. Histological evaluation of CAM tissues

CAM samples were fixed in 5% buffered formalin, embedded in paraffin, sectioned, and stained with (i) hematoxylin and eosin (H&E) for standard histopathological evaluation and (ii) Masson's trichrome to characterize collagen and fibrin deposition within CAM tissues. The stained slides were observed and photographed under a light microscope (Olympus BX50) and analyzed with Image-Pro Plus Software version 4.5.

3. Results and discussion

3.1. Rheological analysis

The extent of formation of xanthan (X) and galactomannan (G) physical hydrogels in X:G mixtures depends on thermodynamic conditions and polymer structures (Dea & Morrison, 1975). Previous studies of the physico-chemical properties of X:G hydrogels determined that stronger interactions occur when xanthan is in a disordered conformation and with high Man:Gal-ratio galactomannans, such as locust bean gum (Bresolin et al., 1997; Bresolin, Milas, Rinaudo, & Ganter, 1998; Bresolin, Milas, Rinaudo, Reicher, & Ganter, 1999). The presence of the ethanolic curcumin solution might affect the interactions between the polysaccharides. If these effects are sufficiently large, then the hydrogel may lose the physical properties that are necessary for pharmaceutical applications (Peppas et al., 2000), so it is important to characterize the rheology of the system.

Polysaccharide solutions are viscoelastic materials – that is, they exhibit solid and liquid characteristics simultaneously, where the elastic and viscous character of a given material is described by the moduli G' and G", respectively. Accordingly, it is possible to quantify the predominance of the solid or liquid character of a sample through dynamic rheology measurements (Iagher, Reicher, & Ganter, 2002; Kavanagh & Ross-Murphy, 1998; Perissutti, Bresolin, & Ganter, 2002). Fig. 1 presents the results of such an analysis, showing frequency sweeps for X:G hydrogels (12.5 g/L total polysaccharide concentration; triangles) and curcumin/X:G hydrogels (12.5 g/L total polysaccharide concentration with 0.5 mg/mL of curcumin; squares). Both samples showed a typical gel-like response, with G' always being significantly larger than G" (within the range of 0.01–10 Hz) and the dynamic viscosity (η^*) decreasing with increasing frequency. Other curcumin/X:G hydrogel samples containing different concentrations of curcumin (0.10–0.5 mg/mL) were tested and exhibited a similar elastic behavior (data not shown).

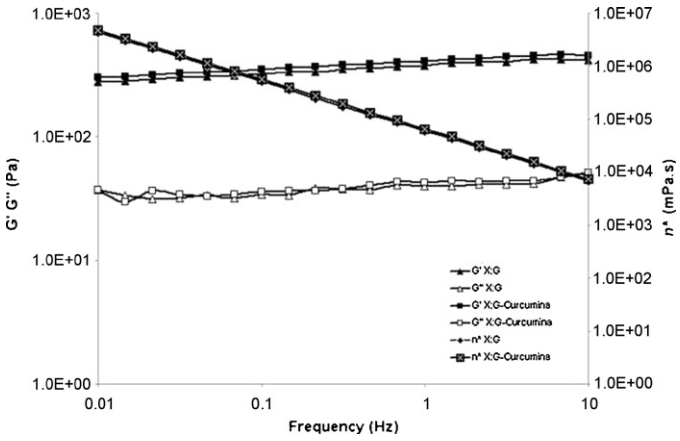

Fig. 1. Frequency dependence of storage modulus (G'), loss modulus (G"), and complex viscosity [η^*] of X:G hydrogels (12.5 g/L) at 25 °C, with and without 0.5 mg/mL of curcumin. G', filled square; G", open square.

The rheological analysis indicates that incorporation of up to 0.5 mg/mL of curcumin did not alter the elastic characteristics of the X:G hydrogel, suggesting that there was no change in the structure of the gel network. A strong, and yet elastic, hydrogel is a very important mechanical characteristic for successful industrial applications (Peppas et al., 2000).

3.2. Release experiments

The release profile of curcumin from X:G hydrogels is presented in Fig. 2. The dissolution profiles show that the curcumin release, measured as curcumin dissolved in the system, increased until reaching a maximum at 5 h, at which point less than 0.5% of incorporated curcumin had been released. The total curcumin concentration in the experiments was about 12 μg/mL, higher than the maximum solubility of curcumin in an aqueous buffer solution (pH 7.4) that was 0.27 μg/mL (Manju & Sreenivasan, 2011). So, is likely that the sink conditions of curcumin/X:G hydrogel system were inadequate, resulting in saturation of the dissolution medium at 5 h; thus, changes to optimize the system, such as the inclusion of surfactants, are needed. However, in order to investigate the probable mechanism at work during the initial 5 h of curcumin release from the hydrogel prior to reaching saturation, we subjected the data to mathematical calculations, applying zero-order, first-order, and Higuchi models. Based on the higher correlation coefficient values (r^2) and less sum of squared residual (SSR) values (Table 1), the release of curcumin from the X:G hydrogel in the first 5 h appeared to satisfy first-order kinetics. Where these conditions apply, the quantity of released drug would be proportional to the amount of

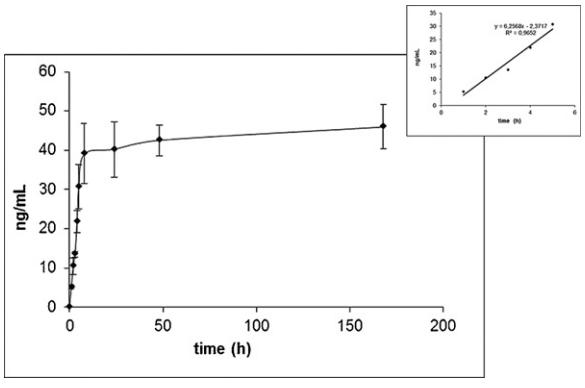

Fig. 2. Profile of curcumin release from X:G hydrogels.

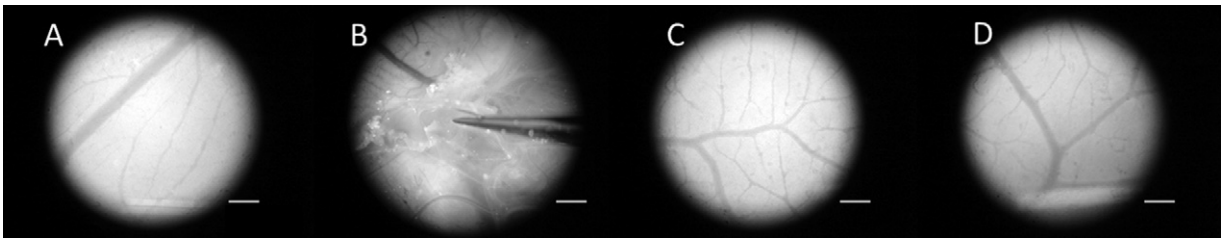

Fig. 3. Gross evaluation of CAM. Photographs of (A) control without implants, (B) PLLA, (C) X:G hydrogel, and (D) curcumin/X:G hydrogel. Note that opacity and fibrosis occurred with PLLA exposure (B), but was not observed with exposure to X:G hydrogel (C) or curcumin/X:G hydrogel (D). The arrowhead indicates the location of PLLA (B). Scale bar: 1 mm.

drug remaining in the interior of the hydrogel, and drug release would decrease with time (Costa, 2002) until the medium became saturated (in this case, at 5 h) and the release of curcumin would stop. In light of the fact that curcumin is a slightly water-soluble drug, other systems must be developed to evaluate the satisfactory sink conditions.

3.3. Chick embryo chorioallantoic membrane (CAM)

3.3.1. Gross evaluation and analysis of angiogenesis in CAM assays

Gross morphological changes induced in the CAM by the biopolymers were examined under a stereomicroscope. Foreign biomaterial applied under the CAM tissue can induce tissue injury and associated tissue responses, namely inflammation and fibrosis. The repair process (wound healing) involves neovascularization or angiogenesis. When inflammatory and repair processes occur in an uncontrolled manner, they lead to extensive tissue destruction, which usually results in tissue fibrosis. In the present study, PLLA films, which induce CAM injury, were used as a positive control. Application of PLLA films alone to the developing CAMs promoted neovascularization, opacity and fibrosis (Fig. 3B). The X:G hydrogel implant and curcumin/X:G hydrogels were completely absorbed after incubating for 1 week and did not provoke tissue injury (Fig. 3C and D); the features of the CAM remained similar to those of the control without implants (Fig. 3A).

An analysis of neovascularization, quantified as VDI (%) as described in Section 2, showed that the number of microvessels in CAMs treated with PLLA films alone significantly increased (279%; $p < 0.05$) compared with untreated controls. The VDI (%) in CAMs treated with the X:G hydrogel trended slightly higher, but this value was not significantly different from those obtained with either the untreated control or the curcumin/X:G hydrogel (Fig. 4).

Gururaj et al. (2002) reported that curcumin, applied on a coverslip and inverted over the CAM, inhibited angiogenesis, reflecting curcumin inhibition of the neovascularization induced by a solid implant. Actually, curcumin attenuates vascular endothelial growth factor (VEGF) overexpression, which occurs in a number of injury conditions (Kunnumakkara et al., 2008). Because the X:G hydrogel did not cause tissue damage (and thus likely did not increase in VEGF expression), the curcumin contained within the X:G hydrogel did not alter the level of vascularization, despite having been released after degradation of the gel. These results show that the X:G hydrogel did not cause tissue injury and the curcumin/X:G hydrogel did not suppress normal vascularization in the *in vivo* CAM model.

3.3.2. Microscopic evaluation of CAM tissues

An examination of representative photomicrographs of histological sections (H&E stained) confirmed an increase in the number of microvessels in CAMs exposed to PLLA (Fig. 5B). Micrographs revealed that X:G hydrogel implants, either without (Fig. 5C) or with (Fig. 5D) curcumin, did not provoke any structural changes in the CAM compared to the controls without implants (Fig. 5A), as evidenced by the absence of an increase in the number of microvessels.

The CAM consists of a mesodermal stroma lined by an outer ectodermal and an inner endodermal. The mesodermal stroma is composed of a complex vasculature supported by thin collagen fibers and fibroblasts. When inflammatory and repair processes occur, they lead to extensive tissue fibrosis. A microscopic evaluation of Masson's trichrome-stained CAMs showed that PLLA increased collagen fibers compared with the control (Fig. 6A). This method stained collagen fibers blue and confirmed that PLLA films induce CAM injury (positive inflammatory control) (Fig. 6B). When the X:G hydrogel and curcumin/X:G hydrogel were placed on top of the CAM for 1 week, implants did not provoke an increase in the production of collagen fibers (Fig. 6C and D), yielding profiles similar to that of the untreated control tissue (Fig. 6A).

Because the CAM model is an appropriate *in vivo* model for simple initial screens of biomaterials and implants (Valdes et al., 2002), we propose that the curcumin/X:G hydrogel is a biocompatible

Table 1
Linear correlation coefficients (r^2), sum of squared residual (SSR), and the angular coefficient (a) obtained from 3 the straight line resulting from the application of mathematical models.

Kinetics models	Parameters	Formulation Curcumin/X:G hydrogel
Zero order	r^2	0.9652
	SSR	14.1020
	a	6.2268
First order	r^2	0.9771
	SSR	0.0431
	a	0.4288
Higuchi model	r^2	0.9608
	SSR	1131.675
	a	19.763

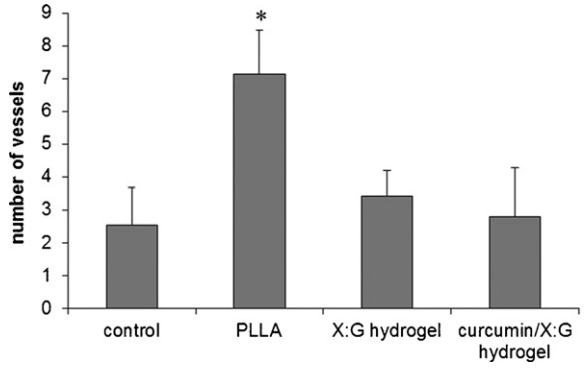

Fig. 4. Graphic representation of the quantitative analysis of angiogenesis, measured as VDI as described in Section 2. Data represent the VDI (%) from six experiments. Vertical bars indicate standard errors. $^*p < 0.05$ *versus* control (Student's *t*-test).

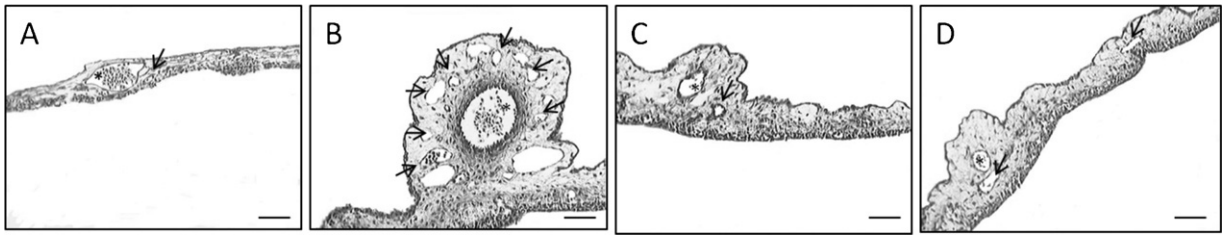

Fig. 5. Representative photomicrographs of histological sections (H&E stained) of CAMs: (A) control (no implants); (B) PLLA; (C) X:G hydrogel; (D) curcumin/X:G hydrogel. Asterisks show branching vessels in the CAM. Arrows indicate positions of microvessels. Scale bar: 100 μm.

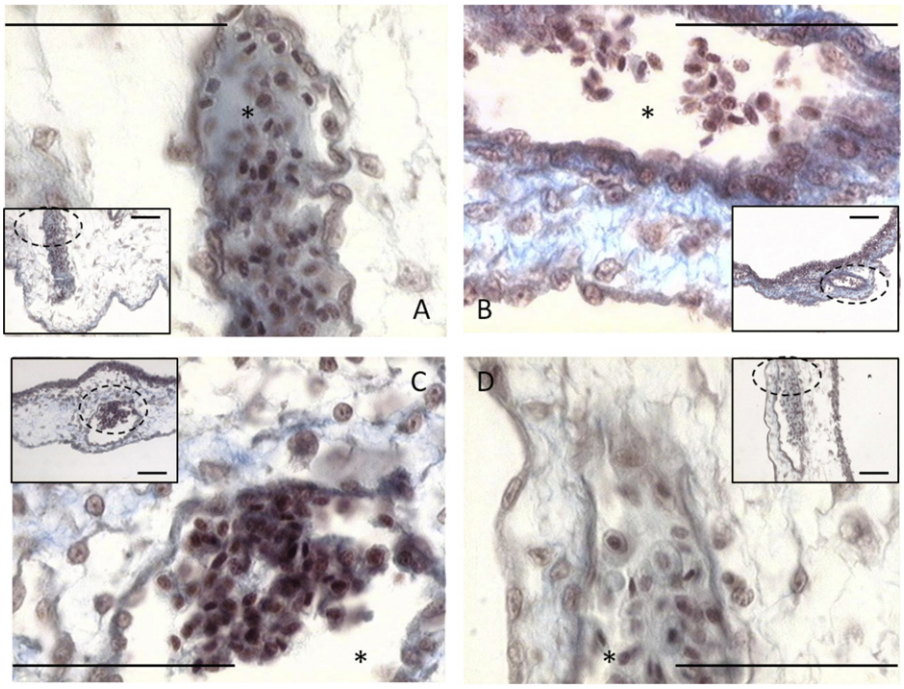

Fig. 6. Histological sections of CAM, stained with Masson's trichrome: (A) control (no implants); (B) PLLA; (C) X:G hydrogel; (D) curcumin/X:G hydrogel. Asterisks indicate vessels in the stroma of the CAM. Scale bar: 50 μm. Dotted lines in insets represent the increased area (8×) that permits observation of collagen fibers (blue). Note the increase in collagen fibers in PLLA-exposed CAMs (B). (For interpretation of the references to color in this figure legend, the reader is referred to the web version of the article.)

material. Gel-dosing forms have been successfully used as drug delivery systems; therefore, future studies will address the kinetics of curcumin release from X:G hydrogels.

4. Conclusion

We can conclude that the incorporation of up to 0.5 mg/mL of curcumin did not alter the elastic characteristics of X:G hydrogels, suggesting that there was no change in the structure of the gel network. The hydrogels remained strong and elastic – two mechanical characteristics that are important for future pharmaceutical, cosmetic, or food applications. We observed no neovascularization or tissue fibrosis after implantation of hydrogels, indicating that X:G hydrogels did not induce tissue injury and suggesting that the curcumin/X:G hydrogel system is highly biocompatible. Therefore, the X:G hydrogel represents a potential matrix for curcumin formulations in various applications, representing a safe system for curcumin delivery.

Acknowledgments

The authors thank Da Granja Agroindustrial Ltd. for providing fertile chicken eggs and Patricia Franchi de Freitas for technical help with CAM assays. The study was financed by CNPq, Nanoglicobiotech-Brazil-MCT/CNPq, PRONEX-Carbohydrates Araucaria Foundation, and Federal University of Paraná-Brazil.

References

Bresolin, T. M. B., Milas, M., Rinaudo, M., & Ganter, J. L. M. S. (1998). Xanthan–galactomannan interactions as related to xanthan conformations. *International Journal of Biological Macromolecules*, *23*(4), 263–275.

Bresolin, T. M. B., Milas, M., Rinaudo, M., Reicher, F., & Ganter, J. L. M. S. (1999). Role of galactomannan composition on the binary gel formation with xanthan. *International Journal of Biological Macromolecules*, *26*(4), 225–231.

Bresolin, T. M. B., Sander, P. C., Reicher, F., Sierakowski, M. R., Rinaudo, M., & Ganter, J. L. M. S. (1997). Viscometric studies on xanthan and galactomannan systems. *Carbohydrate Polymers*, *33*(2-3), 131–138.

Costa, P. J. C. (2002). Avaliação in vitro da lioequivalência de formulações farmacêuticas. *Brazilian Journal of Pharmaceutical Sciences*, *38*(2), 141–153.

Dea, I. C. M., & Morrison, A. (1975). Chemistry and interactions of seed galactomannans. In R. S. Tipson, & H. Derek (Eds.), *Advances in carbohydrate chemistry and biochemistry* (pp. 241–312). Academic Press.

Dorai, T., & Aggarwal, B. B. (2004). Role of chemopreventive agents in cancer therapy. *Cancer Letters*, *215*(2), 129–140.

Eun, J.-P., & Koh, G. Y. (2004). Suppression of angiogenesis by the plant alkaloid, sanguinarine. *Biochemical and Biophysical Research Communications*, *317*(2), 618–624.

Gafner, S., Lee, S.-K., Cuendet, M., Barthélémy, S., Vergnes, L., Labidalle, S., et al. (2004). Biologic evaluation of curcumin and structural derivatives in cancer chemoprevention model systems. *Phytochemistry*, *65*(21), 2849–2859.

Ganter, J. L. M. S., & Reicher, F. (1999). Water-soluble galactomannans from seeds of *Mimosaceae* spp. *Bioresource Technology*, *68*(1), 55–62.

Gururaj, A. E., Belakavadi, M., Venkatesh, D. A., Marmé, D., & Salimath, B. P. (2002). Molecular mechanisms of anti-angiogenic effect of curcumin. *Biochemical and Biophysical Research Communications*, *297*(4), 934–942.

Hazel, S. J. (2003). A novel early chorioallantoic membrane assay demonstrates quantitative and qualitative changes caused by antiangiogenic substances. *Journal of Laboratory and Clinical Medicine*, *141*(3), 217–228.

Iagher, F., Reicher, F., & Ganter, J. L. M. S. (2002). Structural and rheological properties of polysaccharides from mango (*Mangifera indica* L.) pulp. *International Journal of Biological Macromolecules*, *31*(1–3), 9–17. doi:10.1016/s0141-8130(02)00044-2

Jayaprakasha, G. K., Jagan Mohan Rao, L., & Sakariah, K. K. (2005). Chemistry and biological activities of *C. longa*. *Trends in Food Science & Technology*, *16*(12), 533–548.

Kavanagh, G. M., & Ross-Murphy, S. B. (1998). Rheological characterisation of polymer gels. *Progress in Polymer Science*, *23*(3), 533–562.

Klueh, U., Dorsky, D. I., Moussy, F., & Kreutzer, D. L. (2003). Ex ova chick chorioallantoic membrane as a novel model for evaluation of tissue responses to biomaterials and implants [Evaluation Studies]. *Journal of Biomedical Materials Research*, *67*(3), 838–843.

Knighton, D., Ausprunk, D., Tapper, D., & Folkman, J. (1977). Avascular and vascular phases of tumour growth in the chick embryo [Research Support, U.S. Gov't, P.H.S.]. *British Journal of Cancer*, *35*(3), 347–356.

Koop, H. S., Praes, C. E. d. O., Reicher, F., Petkowicz, C. L. d. O., & Silveira, J. L. M. (2009). Rheological behavior of gel of xanthan with seed galactomannan: Effect of hydroalcoholic-ascorbic acid. *Materials Science and Engineering C*, *29*(2), 559–563.

Kunnumakkara, A. B., Anand, P., & Aggarwal, B. B. (2008). Curcumin inhibits proliferation, invasion, angiogenesis and metastasis of different cancers through interaction with multiple cell signaling proteins. *Cancer Letters*, *269*(2), 199–225.

Makri, E. A., & Doxastakis, G. I. (2006). Study of emulsions stabilized with *Phaseolus vulgaris* or *Phaseolus coccineus* with the addition of Arabic gum, locust bean gum and xanthan gum. *Food Hydrocolloids*, *20*(8), 1141–1152.

Manju, S., & Sreenivasan, K. (2011). Conjugation of curcumin onto hyaluronic acid enhances its aqueous solubility and stability. *Journal of Colloid and Interface Science*, *359*, 318–325.

Miquel, J., Bernd, A., Sempere, J. M., Díaz-Alperi, J., & Ramírez, A. (2002). The curcuma antioxidants: pharmacological effects and prospects for future clinical use. A review. *Archives of Gerontology and Geriatrics*, *34*(1), 37–46.

Montembault, A., Viton, C., & Domard, A. (2005). Physico-chemical studies of the gelation of chitosan in a hydroalcoholic medium. *Biomaterials*, *26*(8), 933–943.

Nguyen, M., Shing, Y., & Folkman, J. (1994). Quantitation of angiogenesis and antiangiogenesis in the chick embryo chorioallantoic membrane. *Microvascular Research*, *47*(1), 31–40. doi:10.1006/mvre.1994.1003

Nguyen, K. T., Shaikh, N., Shukla, K. P., Su, S. H., Eberhart, R. C., & Tang, L. (2004). Molecular responses of vascular smooth muscle cells and phagocytes to curcumin-eluting bioresorbable stent materials. *Biomaterials*, *25*, 5333–5346.

Peppas, N. A., Bures, P., Leobandung, W., & Ichikawa, H. (2000). Hydrogels in pharmaceutical formulations. *European Journal of Pharmaceutics and Biopharmaceutics*, *50*(1), 27–46.

Perissutti, G. E., Bresolin, T. M. B., & Ganter, J. L. M. S. (2002). Interaction between the galactomannan from *Mimosa scabrella* and milk proteins. *Food Hydrocolloids*, *16*(5), 403–417.

Roy, A. M., Tiwari, K. N., Parker, W. B., Secrist, J. A., Li, R., & Qu, Z. (2006). Antiangiogenic activity of 4′-thio-β-d-arabinofuranosylcytosine. *Molecular Cancer Therapeutics*, *5*(9), 2218–2224.

Shakibaei, M., John, T., Schulze-Tanzil, G., Lehmann, I., & Mobasheri, A. (2007). Suppression of NF-[kappa]B activation by curcumin leads to inhibition of expression of cyclo-oxygenase-2 and matrix metalloproteinase-9 in human articular chondrocytes: Implications for the treatment of osteoarthritis. *Biochemical Pharmacology*, *73*(9), 1434–1445.

Sharma, R. A., Gescher, A. J., & Steward, W. P. (2005). Curcumin: The story so far. *European Journal of Cancer*, *41*(13), 1955–1968.

Shishodia, S., Chaturvedi, M. M., & Aggarwal, B. B. (2007). Role of curcumin in cancer therapy. *Current Problems in Cancer*, *31*(4), 243–305.

Singh, R. P., & Agarwal, R. (2003). Tumor angiogenesis: a potential target in cancer control by phytochemicals. *Current Cancer Drug Targets*, *3*(3), 205–217.

Srivastava, R. M., Singh, S., Dubey, S. K., Misra, K., & Khar, A. (2011). Immunomodulatory and therapeutic activity of curcumin. *International Immunopharmacology*, *11*(3), 331–341.

Ughini, F., Andreazza, I. F., Ganter, J. L. M. S., & Bresolin, T. M. B. (2004). Evaluation of xanthan and highly substituted galactomannan from *M. scabrella* as a sustained release matrix. *International Journal of Pharmaceutics*, *271*(1–2), 197–205.

Valdes, T. I., Kreutzer, D., & Moussy, F. (2002). The chick chorioallantoic membrane as a novel *in vivo* model for the testing of biomaterials [Research Support, Non-U.S. Gov't, P.H.S.]. *Journal of Biomedical Materials Research*, *62*(2), 273–282.

Vargas, A., Zeisser-Labouèbe, M., Lange, N., Gurny, R., & Delie, F. (2007). The chick embryo and its chorioallantoic membrane (CAM) for the *in vivo* evaluation of drug delivery systems. *Advanced Drug Delivery Reviews*, *59*(11), 1162–1176.

Vendruscolo, C. W., Andreazza, I. F., Ganter, J. L. M. S., Ferrero, C., & Bresolin, T. M. B. (2005). Xanthan and galactomannan (from *M. scabrella*) matrix tablets for oral controlled delivery of theophylline. *International Journal of Pharmaceutics*, *296*(1-2), 1–11.

Xu, M., Deng, B., Chow, Y.-l., Zhao, Z.-z., & Hu, B. (2007). Effects of curcumin in treatment of experimental pulmonary fibrosis: A comparison with hydrocortisone. *Journal of Ethnopharmacology*, *112*(2), 292–299.

Yang, S.-H., Lin, J.-K., Huang, C.-J., Chen, W.-S., Li, S.-Y., & Chiu, J.-H. (2005). Silibinin inhibits angiogenesis via Flt-1, but not KDR, receptor up-regulation1. *Journal of Surgical Research*, *128*(1), 140–146.